Human Genetics (2019) 138:327–337
https://doi.org/10.1007/s00439-019-01990-1

ORIGINAL INVESTIGATION

Novel mutations in *ZP1, ZP2*, and *ZP3* cause female infertility due to abnormal zona pellucida formation

Zhou Zhou[1] · Caixia Ni[2] · Ling Wu[3] · Biaobang Chen[1] · Yao Xu[1] · Zhihua Zhang[1] · Jian Mu[1] · Bin Li[3] · Zheng Yan[3] · Jing Fu[4] · Wenjing Wang[1] · Lin Zhao[1] · Jie Dong[1] · Xiaoxi Sun[4] · Yanping Kuang[3] · Qing Sang[1] · Lei Wang[5,6]

Received: 19 November 2018 / Accepted: 20 February 2019 / Published online: 27 February 2019

Abstract

The human zona pellucida (ZP) is an extracellular glycoprotein matrix composed of ZP1, ZP2, ZP3, and ZP4 surrounding the oocyte, and it plays an important role in sperm–egg interactions during fertilization. Structural and functional changes in the ZP can influence the process of fertilization and lead to female infertility. Previous studies have identified mutations in *ZP1, ZP2*, and *ZP3* that lead to female infertility caused by oocyte degeneration, empty follicle syndrome, or in vitro fertilization failure. Here we describe seven patients from six independent families who had several abnormal oocytes or suffered from empty follicle syndrome, similar to the previously reported phenotypes. By whole-exome sequencing and Sanger sequencing, we identified several novel mutations in these patients. These included three homozygous mutations in *ZP1* (c.1708G > A, p.Val570Met; c.1228C > T, p.Arg410Trp; c.507del, p.His170Ilefs*52), two mutations in a compound heterozygous state in *ZP1* (c.1430 + 1G > T, p.Cys478X and c.1775-8T > C, p.Asp592Glyfs*29), a homozygous mutation in *ZP2* (c.1115G > C, p.Cys372Ser), and a heterozygous mutation in *ZP3* (c.763C > G, p.Arg255Gly). In addition, studies in CHO cells showed that the mutations in *ZP1, ZP2*, and *ZP3* might affect the corresponding protein expression, secretion, and interaction, thus providing a mechanistic explanation for the phenotypes. Our study expands the spectrum of *ZP* gene mutations and phenotypes, and provides a further understanding of the pathogenic mechanism of *ZP* gene mutations in vitro.

Introduction

The human zona pellucida (ZP) is a thick extracellular coat that surrounds the oocyte and is composed of four glycoproteins—ZP1, ZP2, ZP3, and ZP4 (Ganguly et al. 2010; Lefievre et al. 2004). It is critical for the completion of oocyte growth and follicle development (Liu et al. 1996; Rankin et al. 1996, 2001; Wassarman et al. 1998), for sperm–egg interactions during fertilization (Abou-Haila et al. 2014; Wassarman et al. 2001), and for the protection of early embryos prior to implantation (Conner et al. 2005). During fertilization, a sperm initially binds to and penetrates the ZP to fuse with the oocyte and trigger subsequent embryonic development. The ZP restricts interactions between sperm and oocytes from different species

Zhou Zhou and Caixia Ni contributed equally to this manuscript.

Electronic supplementary material The online version of this article (https://doi.org/10.1007/s00439-019-01990-1) contains supplementary material, which is available to authorized users.

✉ Qing Sang
sangqing@fudan.edu.cn

✉ Lei Wang
wangleiwanglei@fudan.edu.cn

[1] State Key Laboratory of Medical Neurobiology, School of Life Sciences and Institutes of Biomedical Sciences, Zhongshan Hospital, Fudan University, Shanghai 200032, China

[2] Center for Reproduction and Genetics, The Affiliated Suzhou Hospital of Nanjing Medical University, Suzhou 215000, China

[3] Reproductive Medicine Center, Shanghai Ninth Hospital, Shanghai Jiao Tong University, Shanghai 200011, China

[4] Shanghai Ji Ai Genetics and IVF Institute, Obstetrics and Gynecology Hospital, Fudan University, Shanghai 200011, China

[5] State Key Laboratory of Genetic Engineering, School of Life Sciences, Zhongshan Hospital, Fudan University, Shanghai 200032, China

[6] Shanghai Center for Women and Children's Health, Shanghai 200062, China

(Claw and Swanson 2012) and prevents fusion of oocytes with more than one sperm in humans (Gupta 2015).

In mice, the ZP is composed of ZP1, ZP2, and ZP3 with a structural model in which ZP1 dimers serve to cross link ZP filaments constructed of ZP2–ZP3 dimers (Rankin et al. 1999; Wassarman et al. 1997). The ZP of oocytes lacking ZP1 proteins was more loosely organized than the ZP surrounding normal oocytes resulting in reduced fecundity (Rankin et al. 1999). Relatively few oocytes were obtained from the oviducts of $Zp2^{-/-}$ mice because the ZP-free oocytes were resorbed even though there was a thin ZP surrounding the preovulatory oocytes (Rankin et al. 2001). Oocytes from $Zp3^{+/-}$ mice had a considerably thinner ZP with reduced levels of both ZP3 and ZP2, but these mice were fertile (Wassarman et al. 1997). However, $Zp3^{-/-}$ female mice failed to form the ZP, although there were still low levels of ZP1 and ZP2 at the surface of the oocytes, and as a result these mice were infertile (Rankin et al. 1996). When the ZP was absent, the cumulus mass was entirely dissociated from the oocyte, resulting in oocyte degeneration (Rankin et al. 1996).

In humans, it was reported that a homozygous frameshift mutation in *ZP1* resulting in a truncated ZP1 protein caused female infertility characterized by the retrieval of ZP-free oocytes for in vitro fertilization (IVF) or the complete absence of oocytes (Huang et al. 2014). A recent study identified two homozygous pathogenic variants (c.1695-2A > G and c.1691_1694dup, respectively) of *ZP2* in infertile patients from two different consanguineous families, and both of these mutations resulted in a thin ZP and IVF failure (Dai et al. 2018). In addition, a heterozygous missense mutation (c.400G > A) in *ZP3* was shown to impede the interaction between ZP2 and ZP3, leading to oocyte degeneration and empty follicle syndrome (Chen et al. 2017).

In this study, we describe seven patients in six unrelated families who received a diagnosis of primary infertility. Most of the oocytes in these patients were degenerated due to the absence of the ZP resulting in difficulty in retrieving oocytes in IVF, which was similar to the reported phenotypes of patients with mutations in *ZP1* and *ZP3*. In addition, several oocytes were retrieved from the proband of family 5 over the course of every IVF cycle, and more than half were devoid of a ZP while the rest exhibited a thin ZP. We identified several novel homozygous and compound heterozygous mutations in *ZP1, ZP2*, and *ZP3*. We also investigated effects of these mutations in vitro.

Materials and methods

Case report

Patients from families 1, 2, and 4 were recruited from Shanghai Ninth Hospital. The patient from family 3 contacted the authors on her own to provide a blood sample and case report. The patients in families 5 and 6 were recruited from the Shanghai Ji Ai Genetics, and IVF Institute and Suzhou Municipal Hospital, respectively. The six probands had normal ovarian reserves and regular menstrual cycles, and their basal sex hormone levels and other infertility-related examinations did not reveal any abnormalities. They received assisted reproduction treatment for one to three cycles but failed to establish a pregnancy. The study was approved by the Ethics Committee of the Medical College of Fudan University and the Reproductive Study Ethics Committee of the Ninth Hospital affiliated with Shanghai Jiao Tong University.

Genomic DNA extraction

All blood samples were isolated and preserved in EDTA tubes after obtaining informed consent from the patients. Genomic DNA was extracted from peripheral blood using the QIAamp DNA Blood Mini Kit (Qiagen), and the DNA concentration and quality were measured with a NanoDrop 1000 spectrophotometer (Thermo Scientific).

Genetic studies

We used a combination of whole-exome sequencing and homozygosity mapping to identify candidate variants in the proband of family 1. Exons of the patient's DNA sample were captured and sequenced with an Illumina HiSeq 2500 instrument. Because the parents of the proband of family 1 were consanguineous, homozygous variants were selected for further analysis. Stringent criteria were applied to exclude the non-pathogenic variants as follows: (1) variants should be located in exonic or splicing regions; (2) variants should present with an allele frequency below 1% in the 1000 Genomes database and the genome Aggregation Database (gnomAD); and (3) the genes should be expressed in all stages of human oocyte development according to our in-house RNA sequencing data of mouse and human oocytes. Homozygosity mapping was performed with HomozygosityMapper to identify candidate homozygous variants that might be located in homozygous regions larger than 1 Mb (Supplemental Fig. 1). Subsequently, the candidate *ZP1* homozygous variant was validated in the patient and in other family members by Sanger sequencing. For the other patients who exhibited a similar phenotype, each exon and its flanking intron sequence of the *ZP1, ZP2*, and *ZP3* genes were amplified and sequenced by Sanger sequencing (Table S1). Previous published papers indicated that mutations in ZP1 and ZP2 displayed a recessive inheritance pattern and the reported ZP3 mutation revealed a dominant inheritance pattern. Female infertility due to zona pellucida defect is a rare genetic disorder whose prevalence is

generally below 0.1%. Therefore, the single allele frequency was 0.1% cut-off for ZP3 in a dominant inheritance pattern. However, the total allele frequency was calculated by the multiplication of both allele frequencies for a single gene in a recessive inheritance pattern. So, when we chose 3% cut-off for ZP1 and ZP2 allele frequency, the total allele frequency was $3\% \times 3\% = 0.09\%$, which was below 0.1% for pathogenic mutation identification. After excluding variants whose allele frequencies were greater than 3% (*ZP1* and *ZP2*) or 0.1% (*ZP3*) in gnomAD, the candidate variants had to be functionally damaging as predicted by SIFT or MutationTaster.

Reverse transcription and amplification of cDNA

Total RNA from granulosa cells of the patient from family 4 and a normal fertile control was extracted with an RNeasy Mini Kit (QIAGEN). After the removal of genomic DNA with gDNA Eraser, reverse transcription was performed with the PrimeScript RT Reagent Kit (Takara). The partial region of *ZP1* cDNA between exon 8 and exon 12 was amplified with the use of specific primers (Table S1) and high-fidelity DNA polymerase KOD-Plus (Toyobo Life Science). Two specific amplified bands of *ZP1* cDNA from the patient were detected through agarose gel electrophoresis and sequenced separately.

Expression vector construction and mutagenesis

The full-length coding sequences of *ZP1, ZP2, ZP3*, and *ZP4* were amplified from cDNA of abandoned GV or MI oocytes. FLAG-tag, MYC-tag, HA-tag, and V5-tag were fused to the N-termini of *ZP1, ZP2, ZP3*, and *ZP4*, respectively, after their signal peptide sequences. These constructs were cloned into the pCMV6-Entry vector (Origene) by SfaAI and MluI (Thermo Scientific) dual-enzyme digestion and were designated as FLAG-ZP1^{WT}, MYC-ZP2^{WT}, HA-ZP3^{WT}, and V5-ZP4^{WT} (Supplemental Fig. 2). Site-directed mutagenesis using the KOD-Plus Mutagenesis Kit (Toyobo Life Science) was performed in the wild-type *ZP1, ZP2*, and *ZP3* expression vectors to introduce the four missense variants p.Val570Met (ZP1), p.Arg410Trp (ZP1), p.Cys372Ser (ZP2), and p.Arg255Gly (ZP3), and these were designated as FLAG-ZP1^{V570M}, FLAG-ZP1^{R410W}, MYC-ZP2^{C372S}, and HA-ZP3^{R255G}, respectively. In addition, untagged human ZP1 expression vectors were constructed for functional assays (Supplemental Fig. 2).

Protein extraction from granulosa cells

Granulosa cells were homogenized in 0.7 mL of QIAzol (Qiagen) and incubated at room temperature (RT) for 5 min. A total volume of 0.14 mL chloroform was added to the homogenate with vigorous shaking for 30 s, incubated at RT for 5 min, and then centrifuged at 12,000×*g* for 10 min. A total volume of 0.2 mL 100% ethanol was added to the interphase and organic phases for DNA precipitation, incubated at RT for 3 min, and centrifuged at 2000×*g* for 5 min at 4 °C. A total volume of 1 mL of isopropanol was added to the phenol–ethanol supernatant, incubated at RT for 10 min, and centrifuged at 12,000×*g* for 10 min at 4 °C to pellet the protein. The protein pellet was washed with 1.4 mL of the wash solution (0.3 M guanidine hydrochloride in 95% ethanol), incubated for 20 min at RT, and then centrifuged at 7500×*g* for 5 min at 4 °C to remove the wash solution, and this was repeated two times. A total volume of 1.4 mL of 100% ethanol was added, incubated for 20 min at RT, and then centrifuged at 7500×*g* for 5 min at 4 °C. After 5 min of air-drying, the protein pellet was suspended in 0.2 mL of 1% SDS, incubated at 50 °C until completely dissolved, and centrifuged at 10,000×*g* for 10 min at 4 °C to sediment and remove insoluble material. The resulting protein sample was then used for western blotting.

Expression of ZP proteins in CHO cells

Chinese hamster ovary cells (CHO cells, supplied by Fudan IBS Cell Center, Shanghai, China) were cultured in Dulbecco's modified Eagle medium (DMEM) supplemented with 10% fetal bovine serum and 1% penicillin/streptomycin (Gibco). CHO cells were transiently transfected with the ZP expression constructs using the PolyJet in vitro DNA transfection reagent (SignaGen). For each 10 cm dish, 10 mL of fresh complete medium with serum and antibiotics was replaced 30 min before transfection. Then 6 μg of ZP plasmids (1.5 μg each of ZP1, MYC-ZP2, HA-ZP3, and V5-ZP4 plasmids) and 18 μL of PolyJet reagent were diluted into 250 μL serum-free DMEM separately. The diluted PolyJet reagent was added to the diluted ZP plasmids immediately, incubated for 15 min at RT, and then added to the 10 cm dish with the growing CHO cells. After 24 h, the complete medium containing PolyJet/DNA complexes was replaced with serum-free DMEM. Secreted proteins were collected after another 24 h. Supernatants were centrifuged at 12,000×*g* for 20 min at 4 °C to sediment cell debris and were then concentrated 50-fold using Amicon Ultra-0.5 centrifugal filter devices (Millipore) according to the manufacturer's protocol. Cell-associated ZP proteins were collected by washing with PBS and incubating for 30 min at 4 °C with 0.5 mL of RIPA lysis buffer (Shanghai Wei AO Biological Technology) supplemented with 1% protease inhibitor cocktail (Bimake). The CHO cells were scraped off the 10-cm dishes and centrifuged at 12,000×*g* for 20 min at 4 °C to sediment the cell debris.

Western blotting

Protein samples were denatured in SDS–PAGE sample loading buffer, heated for 10 min at 95 °C, separated on 10% SDS–PAGE gels, and transferred to a nitrocellulose filter membrane. After 1 h of blocking with 5% nonfat dry milk diluted in phosphate buffered saline with Tween 20, the nitrocellulose membrane was probed with commercially available antibodies specific to ZP1 (against amino acids 40–271, mapping near the N-terminus of human ZP1) (1:500 dilution, Santa Cruz, Cat #: sc-365435), FLAG (1:3,000 dilution, SIGMA, Cat #: F7425), MYC (1:1,000 dilution, CST, Cat #: 2276), HA (1:1,000 dilution, CST, Cat #: 3724), and V5 (1:1,000 dilution, CST, Cat #: 13202) for the detection of recombinant ZP proteins. Rabbit anti-vinculin (1:1,000 dilution, CST, Cat #: 13901) was used as the internal control. The anti-ZP1 antibody mentioned above was also used to detect ZP1 expression in vivo. The secondary antibodies were HRP goat anti-rabbit IgG (1:5000 dilution, Abmart) and HRP goat anti-mouse IgG (1:5000 dilution, Abmart). Some western blotting experiments were replicated for probing the proximal band on the same nitrocellulose membrane. The membranes were stripped with stripping buffer (Shanghai Beyotime Biotechnology, Cat#: P0025B) for 10 min and washed with PBST three times for 5 min before reprobing with another antibody.

Immunoprecipitation

To determine the effects of these missense mutations on the interaction of ZP proteins, CHO cells were transfected with FLAG-ZP1, MYC-ZP2, HA-ZP3, and V5-ZP4 plasmids, and incubated for 36 h. Total protein from transfected cells was extracted in NP-40 lysis buffer (50 mM Tris, 150 mM NaCl, 0.5% NP-40 (pH 7.5), and 1% protease inhibitor cocktail (Bimake)), and immunoprecipitation was performed using anti-FLAG, anti-MYC, or anti-HA beads (Bimake). Western blotting was conducted as described above.

Results

Clinical characteristics of the affected individuals

Six Chinese families were included in this study (Fig. 1). The patient in family 1 was 30 years old, and her parents were first cousins. She had not conceived with unprotected sexual intercourse for 4 years, receiving a diagnosis of primary infertility at the age of 29. The patient in family 2 was 30 years old, and she had not conceived with unprotected sexual intercourse for 6 years, receiving a diagnosis of primary infertility at the age of 28. The patient in family 3 was 28 years old and her parents were first cousins. She had normal menstrual cycles with light dysmenorrhea, receiving a diagnosis of primary infertility after one cycle of IVF. The patient in family four was 33 years old with primary infertility for 6 years. The proband (II-3) of family five came from a consanguineous family. She was 33 years old and had been infertile during 10 years of marriage. Her second sister (II-2) was 34 years old and also had a 6-year history of primary infertility. The patient in family 6 was 29 years old, and she had not conceived with unprotected sexual intercourse for 6 years.

The proband of family 1 had undergone two cycles of IVF. The first cycle failed to obtain any oocytes, and the second cycle retrieved only one oocyte without a ZP from 24 cumulus–oocyte complexes after careful observation (Fig. 2a; Table 1). The proband of family two had three failed IVF attempts, in which only three degenerated oocytes without a ZP were retrieved even though more than 20 follicles were aspirated in each attempt (Table 1). The proband of family three only had one failed attempt in which no oocytes could be obtained from the 24 follicles that were aspirated (Table 1). For the proband of family 4, only ZP-free oocytes were retrieved from three failed IVF attempts (Table 1). The phenotype of the proband in family five (II-3) was different from the other five probands. In addition to several degenerated oocytes, a few mature oocytes with a thin ZP could be retrieved in all three IVF attempts, two of which developed into poor-quality embryos with failed implantation in the first cycle, while the other mature oocytes failed to develop into viable embryos (Fig. 2a, b; Table 1). The phenotype of family member II-2 in family 5 was similar to that of II-3 in family 5. Of note, after four IVF cycles, only one poor-quality embryo was obtained, but this led to a successful pregnancy (the specific clinical information is not available). The proband of family six underwent three failed IVF attempts. Six and two ZP-free oocytes were obtained in her first two cycles, respectively (Table 1), and during her last attempt seven cumulus–oocyte complexes were retrieved, in which only small fragments of ooplasm could be seen (Table 1). In summary, for patients in families 1, 2, 3, 4, and 6, either no oocytes or only ZP-free oocytes were retrieved from the cumulus–oocyte complexes. For the patient (II-3) in family five, ZP-free oocytes and mature oocytes with a thin ZP could be retrieved, but they did not develop normally into viable embryos upon IVF.

Identification of mutations in *ZP1*, *ZP2*, and *ZP3*

Whole-exome sequencing was performed on the patient in family 1. After applying the filtering criteria (See Methods), we identified the single mutation responsible for the phenotype of this patient. This variant, a homozygous missense mutation c.1708G > A (p.Val570Met) in exon 11 of *ZP1* (NM_207341), was predicted to influence protein function

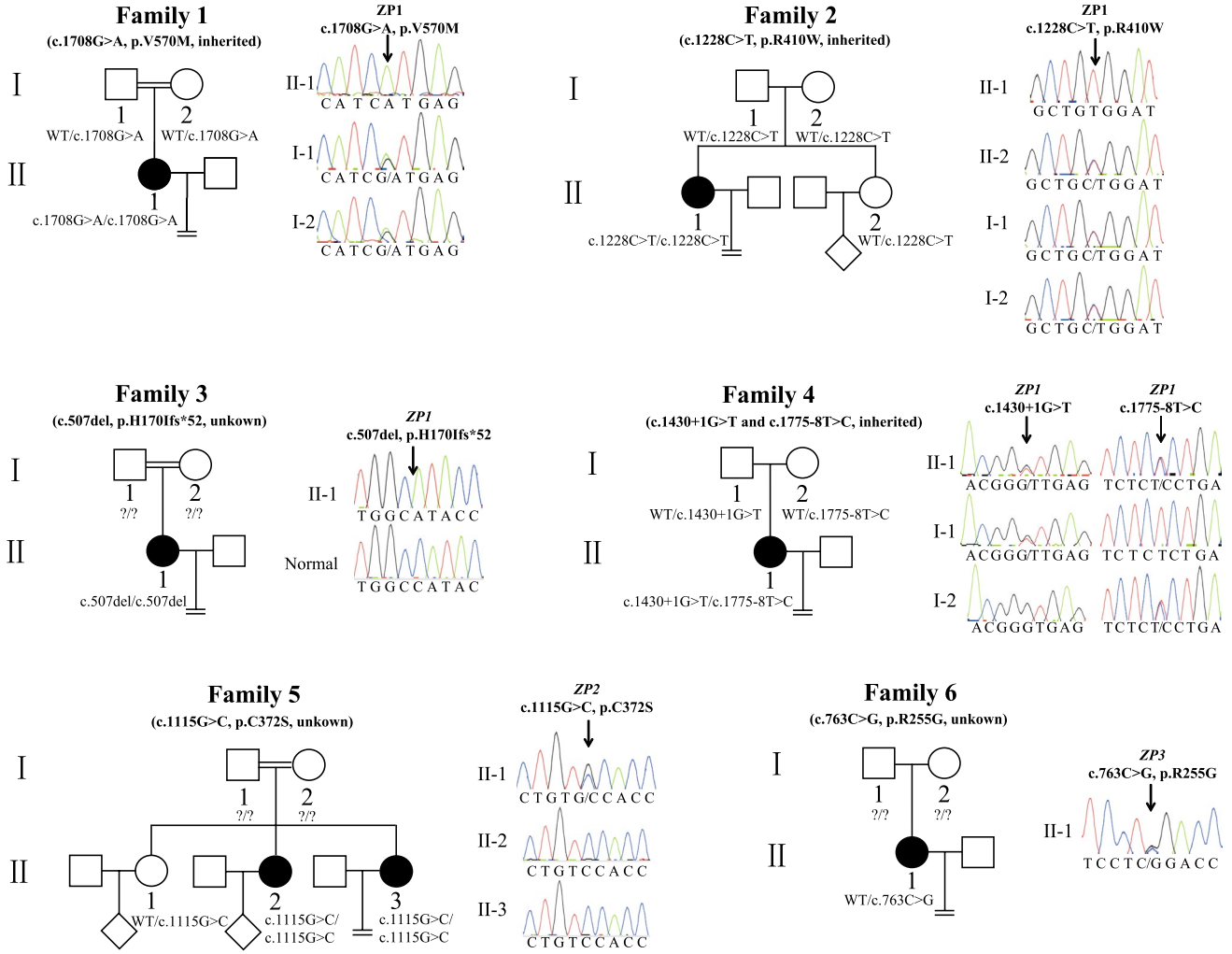

Fig. 1 Identification of mutations in *ZP1, ZP2*, and *ZP3*. Women from six pedigrees presented with abnormal oocyte phenotypes. Families 1, 3, and 5 were consanguineous families. Families 1, 2, 3, 4, and 5 displayed a recessive inheritance pattern, and family six displayed a dominant inheritance pattern. Sanger sequencing confirmation is shown beside the pedigrees. Black circles represent the affected individuals

(Table 2). The mutation was then validated with Sanger sequencing, and both of the patient's parents carried a heterozygous *ZP1* mutation, indicating a recessive inheritance pattern (Fig. 1).

Furthermore, we performed targeted sequencing of *ZP1* in an additional six infertile patients from five independent families who presented with a similar phenotype (Table 1). The proband of family 2 had a homozygous missense mutation c.1228C > T (p.Arg410Trp) in *ZP1* (Fig. 1). A novel homozygous frameshift mutation c.507delC (p.His170Ilefs*52) in *ZP1* was identified in the proband of family 3, and was predicted to result in a truncated protein. In addition, two predicted *ZP1* splicing mutations (c.1430 + 1G > T [p.Cys478X] and c.1775-8T > C [p.Asp592Glyfs*29]) in a compound heterozygous state were found in the proband of family 4 (Fig. 1). To investigate the effects of predicted splicing mutations on mRNA integrity, we amplified and sequenced *ZP1* cDNA from granulosa cells of the patient from family 4 using the specific primers shown in Table S1. With respect to *ZP1* cDNA carrying variant c.1430 + 1G > T, the 69-bp intronic sequence between exon 8 and exon 9 was retained and probably triggered protein truncation, and for *ZP1* cDNA carrying variant c.1775-8T > C the 265-bp intronic sequence between exon 11 and exon 12 was retained and probably resulted in a frameshift and protein truncation (Supplemental Fig. 3a).

However, no mutations in *ZP1* were identified in the probands of family 5 or family 6. Considering that *ZP2* homozygous mutations and *ZP3* heterozygous mutations have been reported to result in thin or missing ZPs, respectively (Chen et al. 2017; Dai et al. 2018), we analyzed family 5 and family 6 to identify novel mutations in *ZP2* or *ZP3*

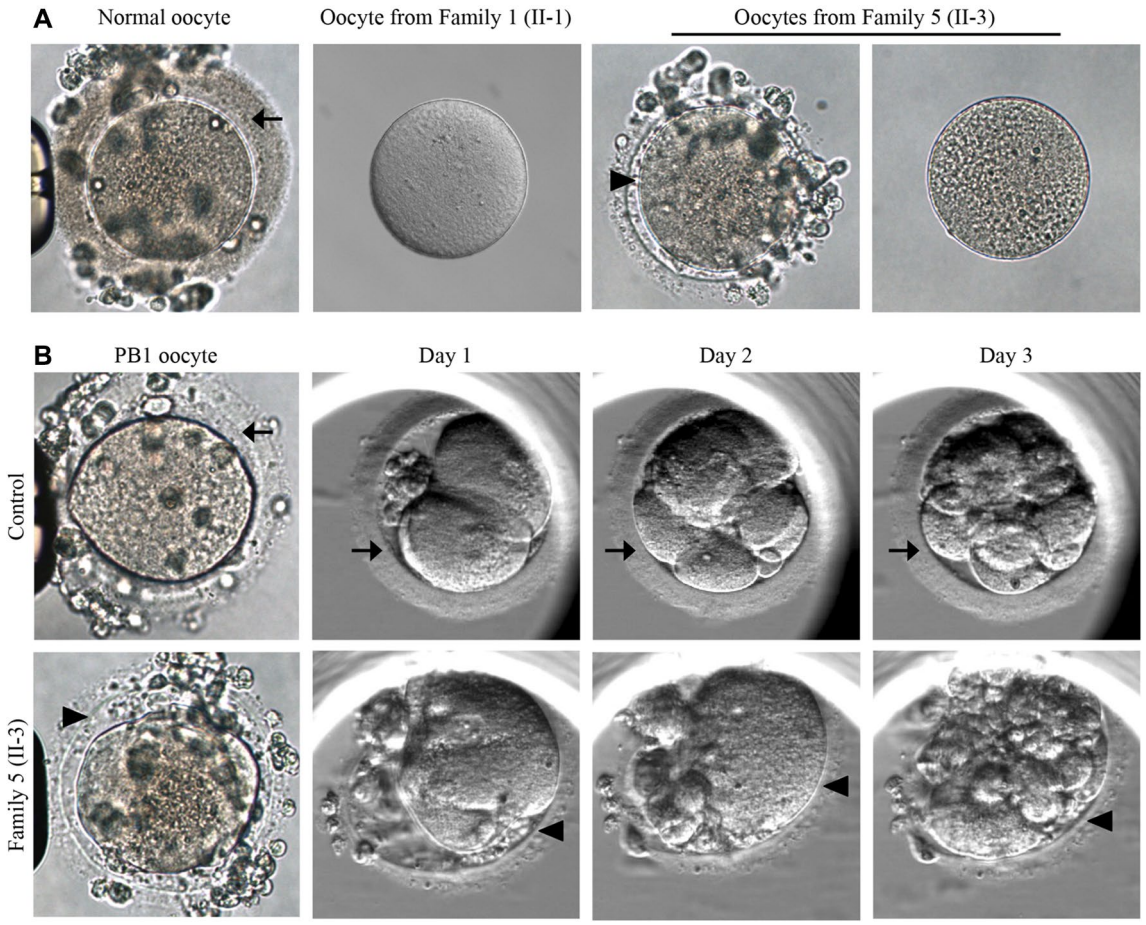

Fig. 2 Phenotypic features of the patients' oocytes. **a** A normal oocyte with surrounding insoluble ZP is shown. Only one ZP-free oocyte was retrieved from the proband of family 1 (II-1). Several ZP-free oocytes and a few mature oocytes with a thin ZP were retrieved from the proband of family 5 (II-3). **b** The mature oocyte with a thin ZP retrieved from the proband of family 5 (II-3) failed to develop into a viable embryo compared to the normal oocyte after 3 days. The black arrow indicates the normal ZP and the black arrowhead indicates the thin ZP

Table 1 Clinical characteristics of the affected individuals and their retrieved oocytes

	Family 1, II-1	Family 2, II-1	Family 3, II-1	Family 4, II-1	Family 5, II-2	Family 5, II-3	Family 6, II-1
Age (years)	30	30	28	33	34	33	29
Duration of infertility (years)	4	6	NA	6	6	10	6
IVF/ICSI cycles	2	3	1	3	4	3	3
Cycle 1							
No. of follicles aspirated	NA	20	24	8	NA	NA	NA
No. of oocytes retrieved	0	0	0	5 ZFOs	NA	3 ZFOs and 2 ZTOs	6 ZFOs
Cycle 2							
No. of follicles aspirated	24	40		10	NA	NA	NA
No. of oocytes retrieved	1 ZFO	0		6 ZFOs	NA	4 ZFOs and 3 ZTOs	2 ZFOs
Cycle 3							
No. of follicles aspirated		20		6	NA	16	7
No. of oocytes retrieved		3 ZFOs		2 ZFOs	NA	4 ZFOs and 1 ZTO	0

IVF in vitro fertilization, *ICSI* intracytoplasmic sperm injection, *NA* not available, *ZFO* ZP-free oocyte, *ZTO* oocyte with a thin ZP

Table 2 Overview of the *ZP* mutations observed in the six families

Mutated gene	Probands in families	Genomic position (bp)	cDNA change	Protein change	Mutation type	Genotype	Inheritance	Phenotype	SIFT	MutTas	gnomAD AF
ZP1	Family 1	chr11:60,642,655	c.1708G > A	p.Val570Met	Missense	Homozygous	AR	Lack of ZP	D	N	2.5×10^{-5}
	Family 2	chr11:60,640,750	c.1228C > T	p.Arg410Trp	Missense	Homozygous	AR	Lack of ZP	D	D	1.3×10^{-5}
	Family 3	chr11:60,637,198	c.507delC	p.His170Ilefs*52	Frameshift Deletion	Homozygous	AR	Lack of ZP	NA	D	8.1×10^{-6}
	Family 4	chr11:60,641,038	c.1430 + 1G > T	p.Cys478X	Splicing	Compound heterozygous	AR	Lack of ZP	NA	D	NA
		chr11:60,642,979	c.1775-8T > C	p.Asp592Glyfs*29	Splicing				NA	NA	4.1×10^{-6}
ZP2	Family 5	chr16:21,213,597	c.1115G > C	p.Cys372Ser	Missense	Homozygous	AR	Thin or lack of ZP	D	D	NA
ZP3	Family 6	chr7:76,063,404	c.763C > G	p.Arg255Gly	Missense	Heterozygous	AD	Lack of ZP	D	D	NA

AR autosomal recessive, *AD* autosomal dominant, *ZP* zona pellucida, *AF* allele frequency in gnomAD database, *NA* not available, *D* damaging, *N* neutral, *NA* not available
Mutation assessment by SIFT and MutationTaster (MutTas)

by sequencing all exons of *ZP2* and *ZP3*. A homozygous missense mutation c.1115G > C (p.Cys372Ser) in *ZP2* was found in the proband (II-3) and her sister (II-2) in family 5, while the fertile oldest sister in family 5 (II-1) had the heterozygous mutation (Fig. 1). A heterozygous missense mutation c.763C > G (p.Arg255Gly) in *ZP3* was found in the proband of family 6 (Fig. 1). Specific information about the mutations is provided in Table 2. The positions of these missense mutations are highly conserved in different mammalian species, and the locations and conservation of *ZP1, ZP2*, and *ZP3* mutations are shown in Fig. 3.

Expression and secretion of mutant protein in cells

To further validate the two splicing mutations identified in family 4, the expression of endogenous ZP1 proteins was detected in the proband of family 4. Because oocytes from the patient were limited, we could only use proteins from granulosa cells to detect ZP1 expression. The relatively decreased endogenous ZP1 proteins in the proband of family 4 might indicate that a majority of predicted truncated ZP1 proteins caused by splicing mutations would be degraded and further impede the normal assembly of the ZP (Supplemental Fig. 3b).

To evaluate the effects of the missense mutations on protein expression and function, CHO cells were co-transfected with four ZP glycoprotein constructs. As indicated by western blot analysis, compared to wild-type ZP proteins the expression of $ZP1^{V570M}$, $ZP1^{R410W}$, and MYC-$ZP2^{C372S}$ was not affected when co-transfected with the other three ZP glycoproteins, while the expression of HA-$ZP3^{R255G}$ was significantly increased, which partially affected the expression of the other co-transfected ZP proteins (Fig. 4 and Supplemental Fig. 4). Subsequently, cell-culture media were collected to detect secreted proteins. Previous studies have shown that after modifications and cleavage by the furin convertases, ZP proteins are secreted from transfected cells into the supernatants and show a shift in migration (Kiefer and Saling 2002; Martic et al. 2004). We found that secreted $ZP1^{WT}$ displayed several diffuse bands, while $ZP1^{V570M}$ and $ZP1^{R410W}$ were nearly undetectable in cell-culture media (Fig. 4a, Supplemental Fig. 4a). MYC-$ZP2^{WT}$ showed two bands, while MYC-$ZP2^{C372S}$ was not secreted into the media, and the other three co-transfected ZP glycoproteins showed no significant differences (Fig. 4b and Supplemental Fig. 4b). These results show that although $ZP1^{V570M}$, $ZP1^{R410W}$, and MYC-$ZP2^{C372S}$ were expressed normally in transfected cells, these mutant proteins were not secreted into the cell-culture media, suggesting possible secretory obstruction and failed assembly of the ZP in vivo. Compared to HA-$ZP3^{WT}$, it seemed that the secretion of HA-$ZP3^{R255G}$ was not impeded (Fig. 4c, Supplemental Fig. 4c).

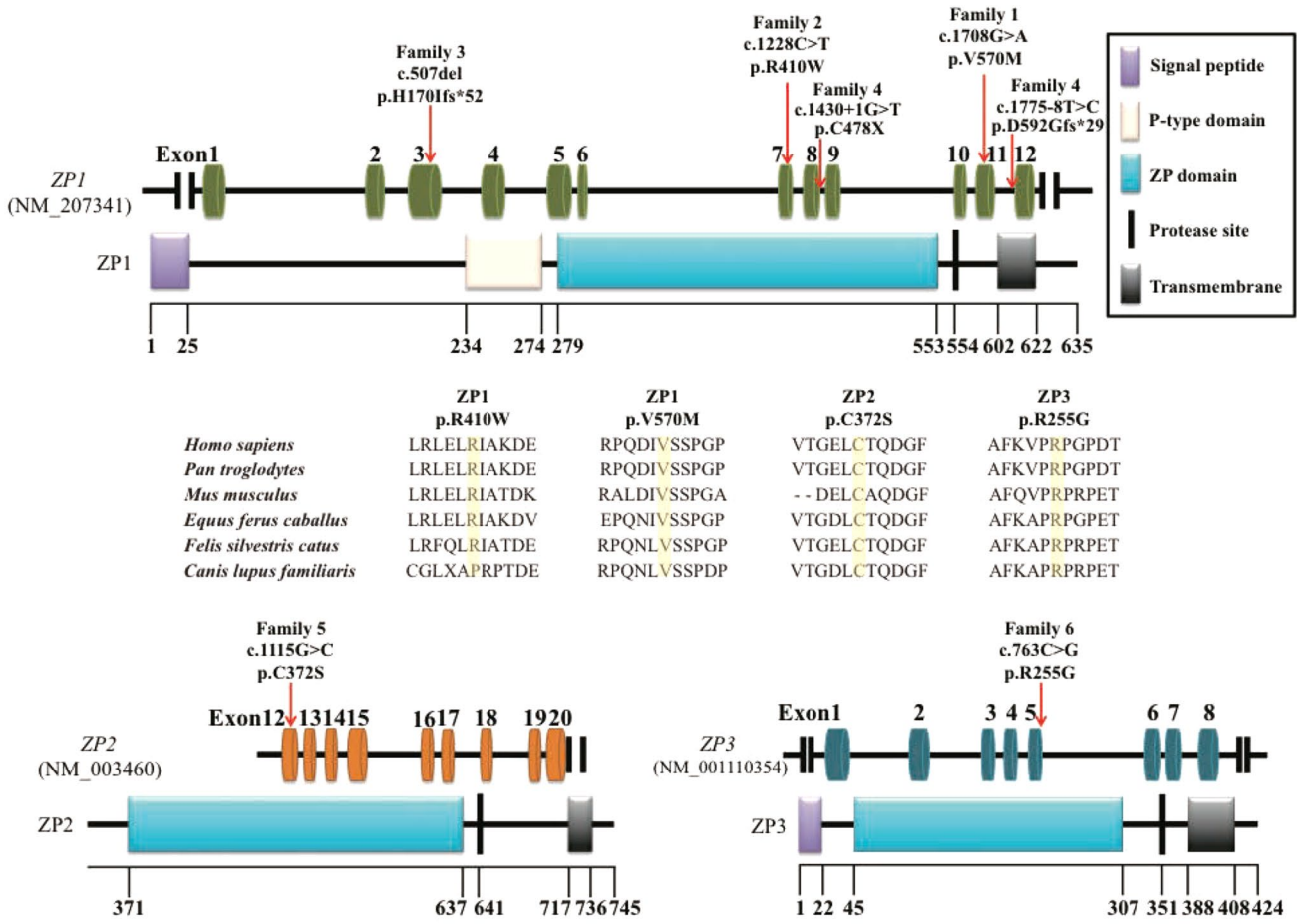

Fig. 3 The locations and conservation of mutated residues in ZP1, ZP2, and ZP3 in mammals. The positions of all mutations are indicated in the genomic structures of *ZP1, ZP2*, and *ZP3* (Gupta et al. 2007), and the conservation of altered amino acids corresponding to missense variants is indicated by the alignment of six mammalian species

In addition, binding of ZP proteins was observed to determine the functions that are affected by the missense mutations. The interactions between mutant ZP1 and ZP2 proteins and the other three wild-type ZP proteins were not affected in vitro (Supplemental Fig. 5a, b, d, e). As for mutant ZP3 proteins, immunoprecipitation experiments suggest that HA-ZP3^{R255G} bound more efficiently to the other three wild-type ZP proteins than HA-ZP3^{WT} (Supplemental Fig. 5c, f).

Discussion

In this study, we recruited seven patients from six independent families with primary infertility. Most of patients had either no oocytes or only ZP-free oocytes in their IVF cycles. Only from the proband of family 5 could a few oocytes with a thin ZP be retrieved in addition to several ZP-free oocytes. Four novel homozygous and compound heterozygous *ZP1* mutations were identified from families 1, 2, 3, and 4; a novel homozygous *ZP2* mutation was identified from family 5; and a novel heterozygous *ZP3* mutation was identified from family 6.

Human ZP3 has been shown to be a homodimer in solution prior to being secreted (Zhao et al. 2004), and human ZP3 and ZP2 are known to traffic independently inside the oocyte because of their cytoplasmic tails that prevent premature aggregation and assembly (Hoodbhoy et al. 2006; Jimenez-Movilla and Dean 2011). Following proteolytic cleavage and secretion, the dormant dimeric ZP3 proteins are disassembled into elongated monomers with conformational changes that allow further interactions between ZP3 and ZP1, ZP2, and ZP4 to form various heterodimeric variants (Kiefer and Saling 2002; Litscher et al. 1999). These building blocks are then assembled into ZP filaments that are interconnected through ZP1 homodimers (Fig. 5a). By combining early research on mouse ZP filaments and current knowledge of the ZP domain architecture, a supramolecular structural model of human ZP has been suggested in which ZP filaments contain structural

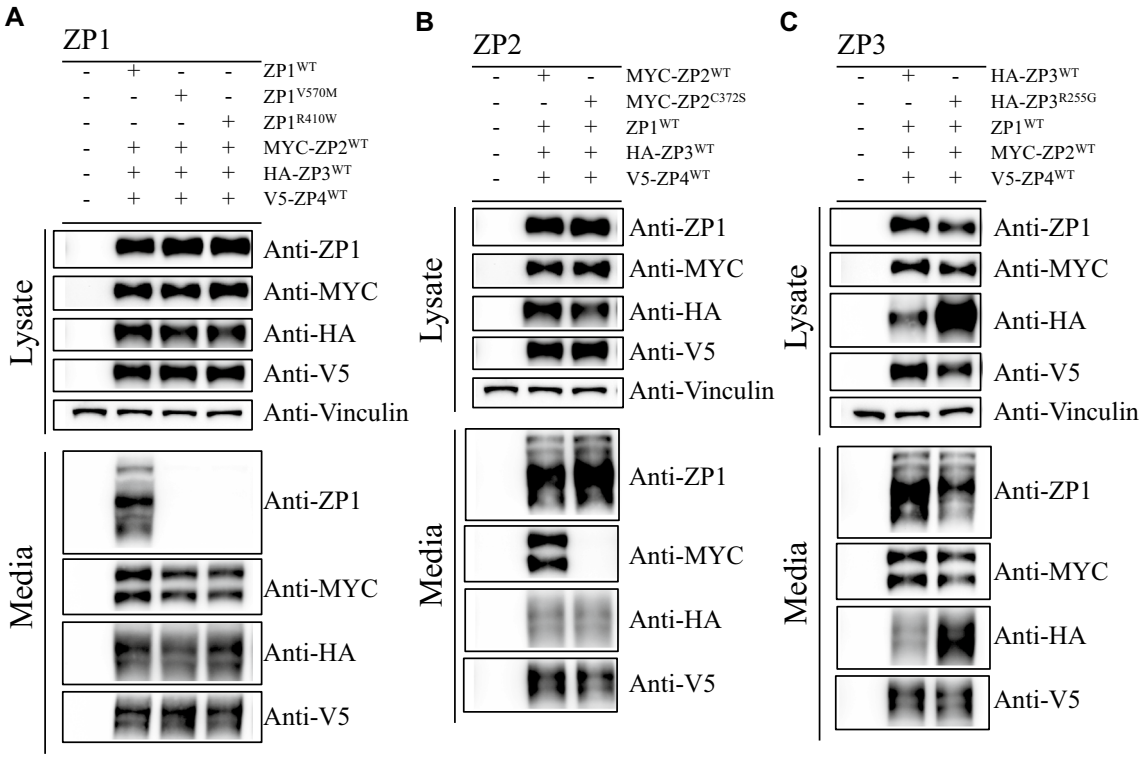

Fig. 4 Effects of the missense mutations on ZP1, ZP2, and ZP3 expression and secretion. **a** Functional study of the missense mutations in *ZP1*. Lanes 2, 3, and 4 show $ZP1^{WT}$, $ZP1^{V570M}$, and $ZP1^{R410M}$ co-transfected with MYC-$ZP2^{WT}$, HA-$ZP3^{WT}$, and V5-$ZP4^{WT}$, respectively. **b** Functional study of the missense mutation in *ZP2*. Lanes 2 and 3 show MYC-$ZP2^{WT}$ and MYC-$ZP2^{C372S}$ co-transfected with $ZP1^{WT}$, HA-$ZP3^{WT}$, and V5-$ZP4^{WT}$, respectively. **c** Functional study of the missense mutation in *ZP3*. Lanes 2 and 3 show HA-$ZP3^{WT}$ and HA-$ZP3^{R255G}$ co-transfected with $ZP1^{WT}$, MYC-$ZP2^{WT}$, and V5-$ZP4^{WT}$, respectively. Cell lysates (upper panel) and media (lower panel) were assayed by immunoblotting using antibodies against ZP1, MYC, HA, and V5. The relevant signals were not detected in untransfected control CHO cells. Vinculin levels ensured protein equivalence among samples. Immunoblots are representative images from experiments that were repeated three times with similar results

repeats constructed of alternating ZP3 and either ZP2 or ZP4, and the less abundant ZP1 occasionally displaces ZP2 and ZP4 to introduce intermolecular cross-links between ZP filaments to stabilize the intact ZP (Bokhove and Jovine 2018; Louros et al. 2016) (Fig. 5a).

Consistent with the function of ZP1 in maintaining the structure of the ZP, a previous study showed that the homozygous frameshift mutation c.1169_1176delTTTTCCCA (p.Ile390Thrfs*16) in *ZP1* prevented the formation of the ZP matrix and resulted in infertility (Huang et al. 2014). In our study, three novel homozygous mutations (c.1708G > A; c.1228C > T; c.507del) and novel compound-heterozygous mutations (c.1430 + 1G > T and c.1775-8T > C) were identified in *ZP1*. No oocytes were retrieved in about half of the IVF cycles of the patients with either the homozygous mutation or the compound-heterozygous mutations in *ZP1* because of oocyte degeneration, and oocytes retrieved from the other cycles of these patients showed no surrounding ZP. These novel mutations might affect the expression or secretion of ZP1 proteins in vivo, thus leading to failure to interconnect the ZP filaments and thus preventing the formation of the ZP (Fig. 5b).

A recent study indicated that patients with homozygous mutations (c.1695-2A > G and c.1691_1694dup) in *ZP2* had a thin ZP devoid of ZP2 proteins (Dai et al. 2018). In the current study, the patients in family 5 with a novel homozygous missense mutation (c.1115G > C) showed a different phenotype. The majority of oocytes retrieved from II-3 had no ZP, while a few oocytes exhibited a thin ZP, among which two poor-quality embryos were formed but failed to implant. The oocytes of her sister (II-2) had a similar phenotype, but the one poor-quality embryo obtained after four IVF cycles was successfully implanted and resulted in a live birth. This observation extends the phenotypic spectrum of patients with *ZP2* variants. The mutated ZP2 proteins might not be secreted to the surface of the oocyte in view of the experimental results in CHO cells, and this might lead to the formation of a thin and defective ZP that only consists of the three other ZP proteins (Fig. 5c).

A recent study identified a heterozygous mutation (c.400G > A) in *ZP3* that caused empty follicle syndrome

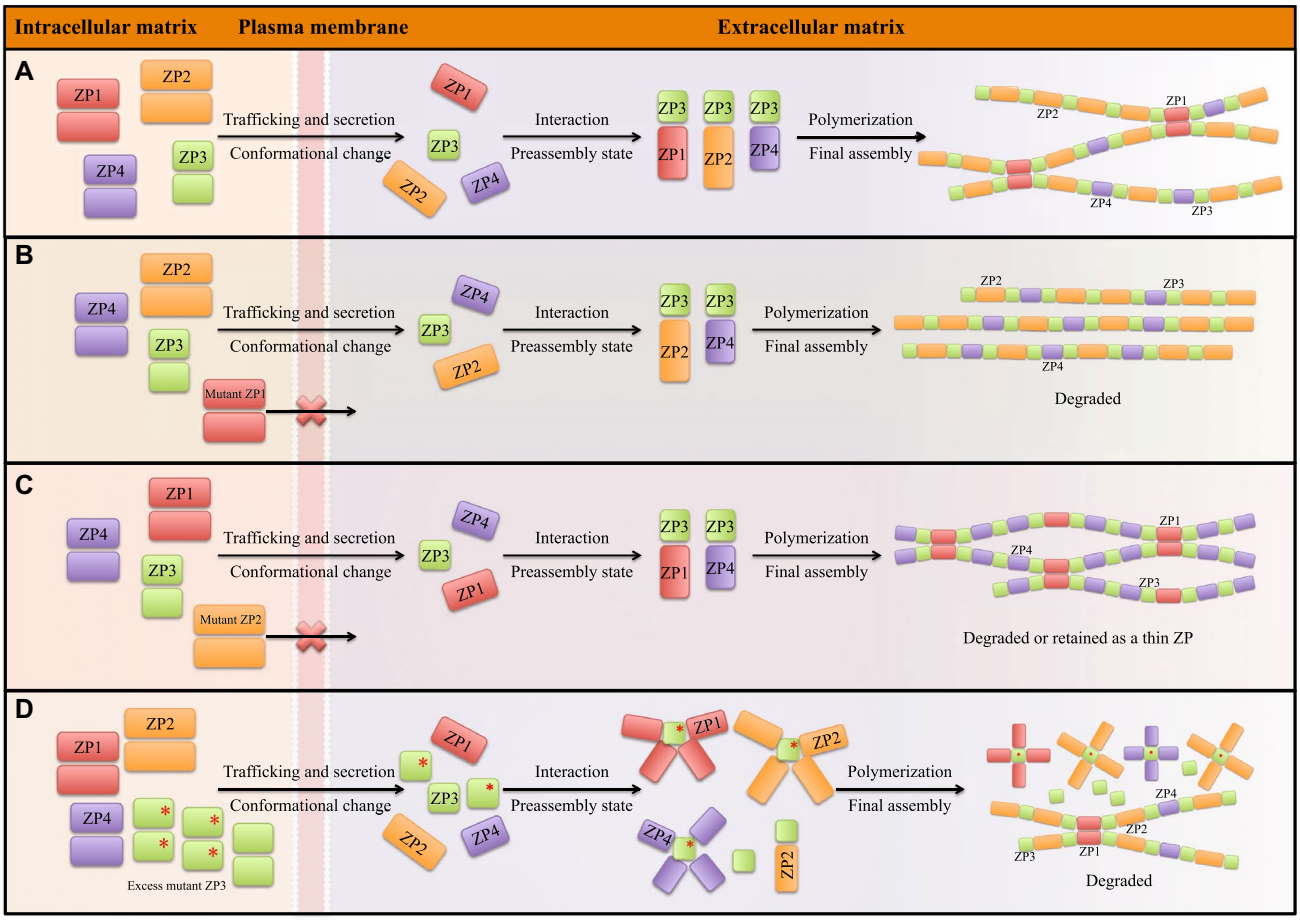

Fig. 5 Potential structures of normal and mutated human ZP. Panel **a** depicts the formation and fine structure of human ZP as hypothesized from the previous studies (Bokhove and Jovine 2018; Hoodbhoy et al. 2006; Huang et al. 2014; Louros et al. 2016; Zhao et al. 2004). Panel **b** shows that ZP filaments devoid of ZP1 dimers fail to interconnect, preventing the formation of the ZP. Panel **c** shows the hypothetical thin ZP structure constructed by glycoproteins ZP1, ZP3, and ZP4. Panel **d** shows the hypothetical pathogenic mechanism of mutated ZP3 proteins (asterisk) in which redundant mutated ZP3 proteins disrupt normal ZP assembly

and female infertility with a dominant inheritance pattern through a dominant-negative effect. In our study, we also identified another heterozygous mutation (c.763C > G) in *ZP3* that has a dominant-negative effect. The expression of mutant ZP3 was significantly increased, producing excess ZP3 proteins in the extracellular matrix. In addition, there could be increased binding affinity between mutant ZP3 proteins and the other three ZP proteins. And mutant ZP3 proteins might compete with wild-type ZP3 proteins for binding to the other three wild-type ZP proteins in vivo, thus impeding the preassembly of heterodimeric variants, while the less abundant heterodimeric variants might be insufficient to construct an ordered and stable ZP surrounding the patient's oocytes (Fig. 5d).

In conclusion, we identified novel mutations in *ZP1*, *ZP2*, and *ZP3* and investigated their effects on the assembly of the ZP in vitro. This study broadens the spectrum of genetic causes and pathogenic mechanisms of human infertility and provides possible diagnostic markers for clinical infertility patients with oocyte retrieval failure, ZP-free oocytes, or oocytes with a thin ZP.

Web Resources

1000 Genomes, http://www.internationalgenome.org/
gnomAD, http://gnomad.broadinstitute.org
DiseaseDX, http://59.110.46.8:3000
HomozygosityMapper, http://www.homozygositymapper.org
SIFT, http://sift.bii.a-star.edu.sg/
MutationTaster, http://mutationtaster.org/MutationTaster/
UCSC, http://genome.ucsc.edu/cgi-bin/hgGateway
Multiple Sequence Alignment, http://www.ebi.ac.uk/Tools/msa/muscle/

Acknowledgements We would like to sincerely thank the patients and their families for their support and participation. This study was supported by the National Key Research and Development Program of China (2017YFC1001500, 2016YFC1000600 and 2018YFC1003800), the National Basic Research Program of China (2015CB943300), the National Natural Science Foundation of China (81725006, 81822019, 81771581, 81571501 and 81771649), the Shanghai Rising-Star Program (17QA1400200) and the Natural Science Foundation of Shanghai (17ZR1401900).

Compliance with ethical standards

Conflict of interest The authors declare no conflict of interest.

Ethics approval The study was approved by the Ethics Committee of the Medical College of Fudan University and the Reproductive Study Ethics Committee of the Ninth Hospital affiliated with Shanghai Jiao Tong University.

Patient consent Obtained.

References

Abou-Haila A, Bendahmane M, Tulsiani DR (2014) Significance of egg's zona pellucida glycoproteins in sperm-egg interaction and fertilization. Minerva Ginecol 66:409–419

Bokhove M, Jovine L (2018) Structure of Zona Pellucida Module Proteins. Curr Top Dev Biol 130:413–442. https://doi.org/10.1016/bs.ctdb.2018.02.007

Chen T et al (2017) A Recurrent Missense Mutation in ZP3 Causes Empty Follicle Syndrome and Female Infertility. Am J Hum Genet 101:459–465. https://doi.org/10.1016/j.ajhg.2017.08.001

Claw KG, Swanson WJ (2012) Evolution of the egg: new findings and challenges. Annu Rev Genomics Hum Genet 13:109–125. https://doi.org/10.1146/annurev-genom-090711-163745

Conner SJ, Lefievre L, Hughes DC, Barratt CL (2005) Cracking the egg: increased complexity in the zona pellucida. Hum Reprod 20:1148–1152. https://doi.org/10.1093/humrep/deh835

Dai C et al (2018) ZP2 pathogenic variants cause in vitro fertilization failure and female infertility. Genet Med. https://doi.org/10.1038/s41436-018-0064-y

Ganguly A, Bansal P, Gupta T, Gupta SK (2010) 'ZP domain' of human zona pellucida glycoprotein-1 binds to human spermatozoa and induces acrosomal exocytosis. Reprod Biol Endocrinol 8:110. https://doi.org/10.1186/1477-7827-8-110

Gupta SK (2015) Role of zona pellucida glycoproteins during fertilization in humans. J Reprod Immunol 108:90–97. https://doi.org/10.1016/j.jri.2014.08.006

Gupta SK, Chakravarty S, Suraj K, Bansal P, Ganguly A, Jain MK, Bhandari B (2007) Structural and functional attributes of zona pellucida glycoproteins. Soc Reprod Fertil Suppl 63:203–216

Hoodbhoy T, Aviles M, Baibakov B, Epifano O, Jimenez-Movilla M, Gauthier L, Dean J (2006) ZP2 and ZP3 traffic independently within oocytes prior to assembly into the extracellular zona pellucida. Mol Cell Biol 26:7991–7998. https://doi.org/10.1128/mcb.00904-06

Huang HL et al (2014) Mutant ZP1 in familial infertility. N Engl J Med 370:1220–1226. https://doi.org/10.1056/NEJMoa1308851

Jimenez-Movilla M, Dean J (2011) ZP2 and ZP3 cytoplasmic tails prevent premature interactions and ensure incorporation into the zona pellucida. J Cell Sci 124:940–950. https://doi.org/10.1242/jcs.079988

Kiefer SM, Saling P (2002) Proteolytic processing of human zona pellucida proteins. Biol Reprod 66:407–414

Lefievre L et al (2004) Four zona pellucida glycoproteins are expressed in the human. Hum Reprod 19:1580–1586. https://doi.org/10.1093/humrep/deh301

Litscher ES, Qi H, Wassarman PM (1999) Mouse zona pellucida glycoproteins mZP2 and mZP3 undergo carboxy-terminal proteolytic processing in growing oocytes. Biochemistry 38:12280–12287

Liu C, Litscher ES, Mortillo S, Sakai Y, Kinloch RA, Stewart CL, Wassarman PM (1996) Targeted disruption of the mZP3 gene results in production of eggs lacking a zona pellucida and infertility in female mice. Proc Natl Acad Sci U S A 93:5431–5436

Louros NN, Chrysina ED, Baltatzis GE, Patsouris ES, Hamodrakas SJ, Iconomidou VA (2016) A common 'aggregation-prone' interface possibly participates in the self-assembly of human zona pellucida proteins. FEBS Lett 590:619–630. https://doi.org/10.1002/1873-3468.12099

Martic M et al (2004) Recombinant human zona pellucida proteins ZP1, ZP2 and ZP3 co-expressed in a human cell line. Asian J Androl 6:3–13

Rankin T et al (1996) Mice homozygous for an insertional mutation in the Zp3 gene lack a zona pellucida and are infertile. Development 122:2903–2910

Rankin T, Talbot P, Lee E, Dean J (1999) Abnormal zonae pellucidae in mice lacking ZP1 result in early embryonic loss. Development 126:3847–3855

Rankin TL, O'Brien M, Lee E, Wigglesworth K, Eppig J, Dean J (2001) Defective zonae pellucidae in Zp2-null mice disrupt folliculogenesis, fertility and development. Development 128:1119–1126

Wassarman PM, Qi H, Litscher ES (1997) Mutant female mice carrying a single mZP3 allele produce eggs with a thin zona pellucida, but reproduce normally. Proc Biol Sci 264:323–328. https://doi.org/10.1098/rspb.1997.0046

Wassarman PM, Liu C, Chen J, Qi H, Litscher ES (1998) Ovarian development in mice bearing homozygous or heterozygous null mutations in zona pellucida glycoprotein gene mZP3. Histol Histopathol 13:293–300

Wassarman PM, Jovine L, Litscher ES (2001) A profile of fertilization in mammals. Nat Cell Biol 3:E59–E64. https://doi.org/10.1038/35055178

Zhao M et al (2004) Mass spectrometry analysis of recombinant human ZP3 expressed in glycosylation-deficient CHO cells. Biochemistry 43:12090–12104. https://doi.org/10.1021/bi048958k